International Journal of Mass Spectrometry and Ion Processes 128 (1993) 181–194
0168-1176/93/$06.00

Absolute cross sections for the dissociative electron impact ionization of the CF_x ($x = 1-3$) free radicals

V. Tarnovsky, P. Kurunczi, D. Rogozhnikov†, K. Becker*

Physics Department, City College of the City University of New York, New York, NY 10031, USA

(Received 30 April 1993; accepted 17 June 1993)

Abstract

We studied the dissociative ionization of the CF_x ($x = 1-3$) free radicals by electron impact and measured absolute partial cross sections and appearance energies for the formation of the various fragment ions. Fast beams (3–3.5 kV) of CF_3, CF_2 and CF were prepared by near-resonant charge transfer of CF_3^+, CF_2^+ and CF^+ with Xe under conditions where the neutral beams contained primarily ground state ions with little vibrational excitation (0.5 eV or less). Absolute cross sections for the various molecular fragment ions were measured from threshold to 200 eV with peak cross sections of up to 1.3 Å^2. The cross sections for the formation of the atomic C^+ and F^+ ions were found to be small (0.3 Å^2 or less) except for the F^+ cross section from CF_2. The measured appearance energies indicate that the fragment ions are formed with excess kinetic energies ranging from essentially zero to about 3 eV per fragment. The CF^+ cross section from CF_2 shows a second onset which corresponds to the double positive ion formation $CF_2 \rightarrow CF^+ + F^+$. Extensive ion trajectory calculations were carried out in order to quantify the collection efficiency of our apparatus for fragment ions formed with excess kinetic energy.

Key words: Electron impact ionization; Electron collision cross sections; Free radicals; Plasma processing

Introduction

The CF_4 molecule is frequently used in feedstock gas mixtures that are employed in the plasma-assisted etching of SiO_2 [1,2]. CF_4 and its free radicals CF_3, CF_2 and CF play an important role in the complex surface chemistry that occurs in the SiO_2 etching process [2–4]. In a conventional plasma reactor the flux of species that impact on the surface that is to be etched is determined by the gas phase reactions in the processing plasma. Experimental and theoretical studies aimed at improving our understanding of the electronic and atomic collision processes involving the CF_4 molecule and the CF_x ($x = 1-3$) free radicals have received considerable attention in recent years. Most experimental and theoretical efforts have focused on the stable CF_4 molecule (see e.g. Müller et al. [5], Iga et al. [6] and references cited therein). The electron-impact ionization of CF_4 has been studied recently by Bruce and Bonham [7] and by Poll et al. [8] who measured the absolute ionization cross section for the parent molecule as well as for the formation of the various fragment ions. In addition, Bruce et al. [9] studied the positive ion pair production by dissociative electron impact ionization of CF_4. Collision studies involving the free radicals CF_3, CF_2 and CF are scarce. Tarnovsky and Becker [10] recently reported absolute parent ionization cross sections for these species using the fast-neutral-beam

* Corresponding author.
† High School Summer Intern, John F. Kennedy High School, New York.

technique. Dissociative ionization processes are more difficult to study, since the fragment ions can be formed with excess kinetic energies which can affect the complete extraction of the product ions from the interaction region and/or interfere with the transport and the collection of all product ions [7,8,11].

In this paper we report absolute partial cross sections for the formation of the various fragment ions produced by dissociative ionization of the free radicals CF_3, CF_2 and CF. Absolute ionization cross sections were measured in our fast-beam apparatus from threshold to 200 eV for singly positively charged fragment ions. Detailed studies of the near-threshold regions were carried out in an effort to determine the appearance energy for each ion. A comparison of the measured appearance energy for a particular ion with the thermochemically and spectroscopically determined minimum energy required for the formation of that fragment ion can provide information about the excess kinetic energy that is released in the process and carried away by the dissociating fragments. Extensive ion trajectory calculations using the SIMION software package [12] have been carried out in an effort to quantify the capability of our apparatus to collect fragment ions formed in the interaction region with a certain amount of excess kinetic energy. Up to now, experimental studies of the dissociative electron impact ionization of free radicals have been extremely scarce. The first studies along these lines were carried out by Biaocchi et al. [13] for CD_3 and CD_2. Further measurements by the same group focused on the electron-impact ionization and dissociative ionization of SiF_x ($x = 1$–3) radicals [14–16] in addition to some earlier preliminary studies in CF_3 [17]. Calculations of total single ionization cross sections of the SiF_x radicals have been carried out by Deutsch et al. [18] using a new approach which reproduced the anomaly in the SiF_x cross section ordering. Preliminary accounts of some of the results discussed in this paper have already been presented at conferences [11,19,20].

Experimental

The crossed-electron-beam–fast-neutral-beam apparatus used in the present experiments, the characteristics of its performance, a comprehensive analysis of potential sources of systematic uncertainties in the experimental procedure and an estimate of the overall accuracy of the measured cross sections have been described in full detail in previous publications [21–23]. We will only give a brief summary and highlight those aspects of the apparatus and the procedure that are specific to the investigation of dissociative ionization processes. A schematic diagram of the apparatus is shown in Fig. 1.

A 3–3.5 kV fast neutral beam of either CF_3, CF_2 or CF radicals is prepared by near-resonant charge transfer of the respective primary mass selected ion beam with Xe. After the remaining ions have been removed from the beam by electrostatic deflection and after most molecules in Rydberg states have been field ionized and deflected, the remaining neutral beam passes through a beam-defining aperture before it is crossed with a well-characterized electron beam (beam energy 5–200 eV, beam current 20–400 μA). The neutral beam is monitored by a secondary emission detector and its flux can be determined in absolute terms by a cali- brated pyroelectric detector. The product ions are focused in the entrance plane of an electrostatic hemispherical analyzer which separates ions of different energy as well as separating the ions from the neutrals. The ions are detected by a channel electron multiplier with a 25 mm entrance cone mounted directly behind the exit plane of the hemispherical analyzer. As discussed in the previous paper on the parent ionization of the CF_x radicals [10], the experimental conditions could be optimized so that the neutral beams contained essentially only ground state neutral radicals with little, if any, vibrational excitation (0.5 eV or less).

The fast-beam apparatus was originally designed for ionization cross section measurements of atomic targets and for the parent ionization of

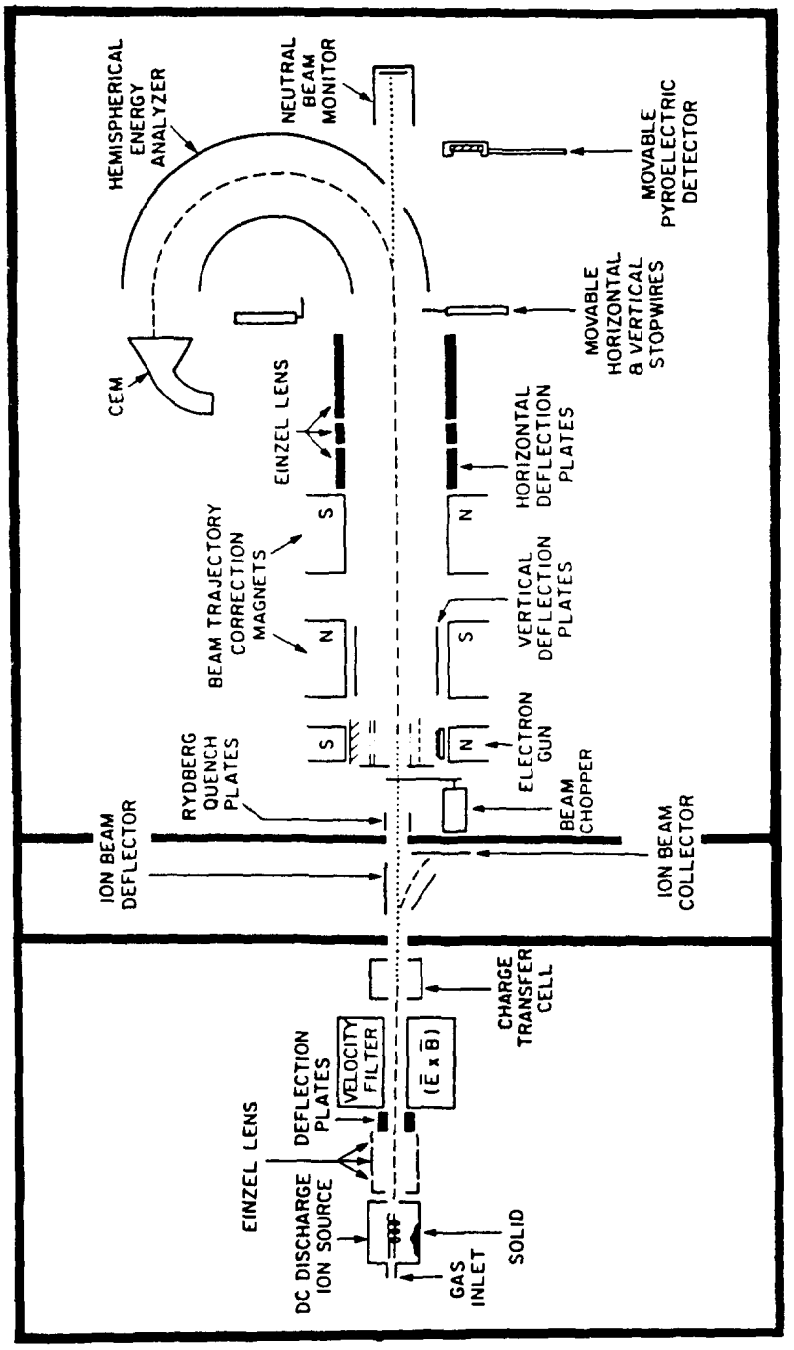

Fig. 1. Schematic diagram of the fast-beam apparatus.

molecules. The momentum imparted to the target by the ionizing electron in this case is negligible, so that the product ions essentially retain the tight collimation of the fast neutral beam which, in turn, enables the collection of the product ions with essentially 100% efficiency. The beam trajectory correction magnets (see Fig. 1) facilitate a re-direction of the product ions which are deflected slightly in the interaction region by the magnetic field that is used to collimate the electron beam. The electrostatic Einzel lens re-focuses the product ion beam emerging from the interaction region in the entrance plane of the hemispherical analyzer to a well-defined spot of spatial extent 0.25 mm or less and small angular divergence, so that no ions will strike the walls of the hemispherical analyzer and no ions will be lost from the ion flux reaching the CEM detector [10]. The situation is more complicated for dissociative ionization processes where the fragment ions in the interaction region can be formed with a certain amount of excess kinetic energy which causes the product ions to spread out spatially. As a result, product ions may be lost (see discussion below) which will affect the measured ion count rate and the cross section deduced from it.

There are four areas between the interaction region and the ion detector in our fast-beam apparatus where product ions with excess kinetic energy might be lost: (1) in the interaction region; (2) in the Einzel lens; (3) in the hemispherical analyzer; (4) at the entrance to the CEM detector (see Fig. 1). Extensive ion trajectory modelling using the SIMION software package [12] was carried out to investigate and to quantify — to the maximum extent possible — ion losses for the processes under investigation [11]. The model calculations assumed a two-fragment break-up of a CF_3, CF_2 or CF molecular radical travelling at a fixed incident velocity (corresponding to 3.0–3.5 kV) in a spatially extended interaction region into the ionic fragment under investigation and a corresponding second neutral fragment with a fixed (but arbitrarily chosen and variable) excess kinetic energy assuming a random angular distribution of the fragments in the center-of-mass system. In the laboratory frame, the fragment ions are spread out in a cone along their flight path. The (maximum) solid angle of this cone is determined by the ratio of the masses of the two dissociating fragments (for fixed incident energy and a fixed value of the excess kinetic energy). The trajectories of the ionic fragments were calculated from the interaction region through the Einzel lens and the hemispherical analyzer to the entrance cone of the CEM. Excess kinetic energies in our simulation were varied from essentially zero to more than 10 eV per fragment (which was considerably higher that the typical excess energies for the processes under investigation as determined from appearance energy measurements carried out as part of our studies; see discussion below). We note that in the absence of any internal excitation of the dissociation fragments the excess kinetic energies E_1 and E_2 of the two dissociating fragments in the two-fragment break-up of a parent molecule/radical are related to the total excess kinetic energy E^{tot} (the quantity determined in the appearance energy measurements) through the relations

$$E_1 = E^{tot}(m_2/M) \tag{1a}$$

and

$$E_2 = E^{tot}(m_1/M) \tag{1b}$$

and the two fragment energies are related to one another by

$$(E_1/E_2) = (m_2/m_1) \tag{1c}$$

Here m_1 and m_2 denote the masses of the two fragments and M, given by $M = m_1 + m_2$, refers to the total mass of the parent molecule/radical. The modeling of the three-fragment break-up of e.g. CF_3 into $CF^+ + F + F$ was not carried out, since the distribution of the excess kinetic energy among the three fragments enters into the problem as an unknown variable which is difficult to handle. The modeling results can be summarized as follows.

(1) No product ions are lost in the interaction region as long as the excess kinetic energy per

fragment is not unrealistically large (15 eV or more).

(2) Product ions leaving the interaction region with excess energies of not more than 10 eV per fragment for the molecular fragment ions CF_2^+ and CF^+ and less than about 6 eV per fragment for the atomic fragment ions C^+ and F^+ will be re-focused by the Einzel lens (which has an inner diameter of 63.5 mm). For larger excess kinetic energies, some of the ions will hit the central element of the Einzel lens and be lost from the product ion flux.

(3) The most likely area where product ions will be lost is inside the hemispherical analyzer (which has a spacing of 38 mm between the inner and the outer hemisphere; see Fig. 1). Even a fraction of the product ions which are re-focused by the Einzel lens can hit the inner walls of the hemispherical analyzer. As discussed before, the fragment ions in the laboratory frame are spread out in a cone along their flight path. This results in a transverse energy component ranging from 0 eV to a maximum value which is determined by the (maximum) solid angle of the cone in addition to the spread in the longitudinal ("beam") energy caused by the excess kinetic energy. Even though ions with different transverse and longitudinal energies can be re-directed by the Einzel lens, they cannot be re-focused to a spatially narrow spot ("tight focus"). At best, the product ions can be re-directed to a spatially extended spot ("weak focus"), which, in turn, causes a spread of the ion trajectories along their further path inside the electrostatic hemispherical analyzer. It was found that for certain combinations of excess kinetic energy, fragment ion mass and Einzel lens focusing voltage up to 50% of the product ions which were "re-focused" by the Einzel lens were lost in the hemispherical analyzer. It was also found that the ion loss in the hemispherical analyzer was minimized when the position of the weak focus of the product ions was not in the entrance plane of the hemispherical analyzer (which was the case for the tight focusing conditions used in the atomic and molecular parent ionization cross section measurements [10,23]), but rather at a position further inside the hemispherical analyzer. This result of the trajectory modeling was easily verified experimentally by monitoring the ion signal detected by the CEM as a function of the Einzel lens focusing voltage. Maximum throughput was observed for Einzel lens voltages which did not correspond to a re-focusing of the product ions in the entrance plane of the hemispherical analyzer. We also note that the major ion loss inside the hemispherical analyzer typically does not occur near the analyzer exit. Depending on the exact focusing conditions, the ion trajectory distribution is widest at an earlier stage of the ion flight path through the hemispherical analyzer. Figure 2 shows the calculated transmission of CF_2^+ fragment ions from the parent CF_3 radical through the hemispherical analyzer as a function of the total excess kinetic energy (lower energy scale). Also indicated in Fig. 2 is the excess kinetic energy per CF_2^+ fragment which is shown on the upper energy scale. The relationship between the two energy scales follows immediately from Eq. (1a) with $M = 69$ u and $m_2 = 19$ u. It is obvious that no significant ion loss occurs as long as the excess kinetic energy per CF_2^+ fragment is below 4.5 eV, which corresponds to a total excess kinetic energy of about 17 eV. Figure 3 shows the

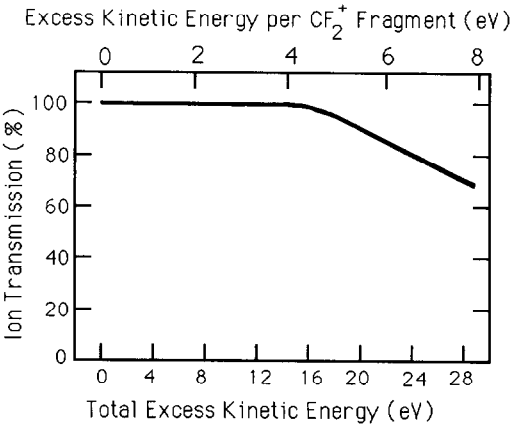

Fig. 2. Ion transmission of CF_2^+ fragment ions produced in the two-fragment break-up $CF_3 \rightarrow CF_2^+ + F$ through the hemispherical analyzer as a function of the total excess kinetic energy (lower energy scale). Also indicated is the excess kinetic energy per CF_2^+ fragment (upper energy scale).

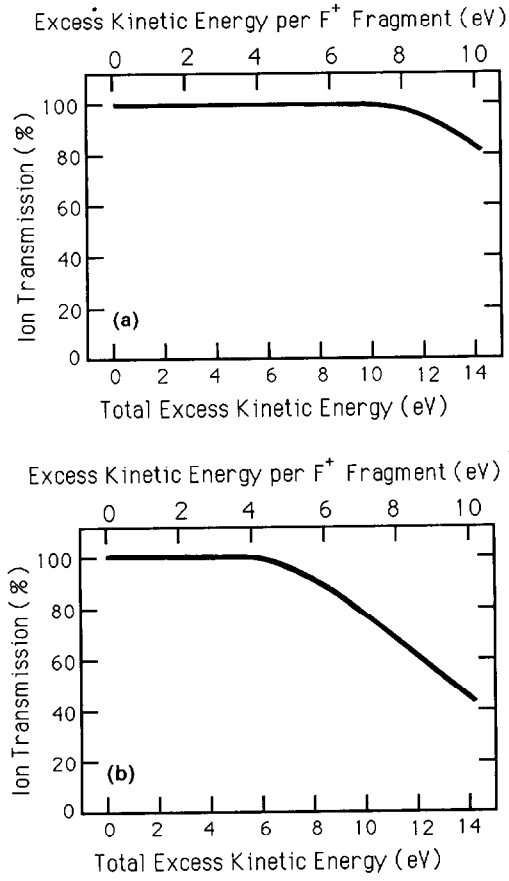

Fig. 3. (a) Ion transmission of F^+ fragment ions produced in the two-fragment break-up $CF_3 \rightarrow CF_2 + F^+$ through the electrostatic Einzel lens as a function of the total excess kinetic energy (lower energy scale). Also indicated is the excess kinetic energy per F^+ fragment (upper energy scale). (b) Same as (a) for the ion transmission of F^+ fragment ions through the hemispherical analyzer.

calculated ion transmission of F^+ ions from CF_3 through the Einzel lens (Fig. 3(a)) and through the hemispherical analyzer (Fig. 3(b)) as a function of the total excess kinetic energy and the excess kinetic energy per F^+ fragment. Here ion losses can occur in the Einzel lens for excess kinetic energies per fragment of 7 eV or more. Significant ion losses in the hemispherical analyzer occur for excess kinetic energies per fragment as low as 4 eV. This corresponds to a much smaller total excess kinetic energy of only about 5.5 eV for the two-fragment break-up of the parent CF_3 radical because of the mass ratio that appears in Eq. (1a). Furthermore, the F^+ ion loss increases much more rapidly with increasing excess kinetic energy compared to the CF_2^+ ion loss (cf. Fig. 2).

(4) There is little, if any, loss of fragment ions between the exit of the hemispherical analyzer and the entrance cone of the CEM detector. More than 95% of all fragment ions leaving the hemispherical analyzer will enter the CEM entrance cone in essentially all cases.

Table 1 summarizes the modeled ion transmissions for several typical processes that were studied in this work. For each process, ion trajectory modeling calculations were carried out for various total excess kinetic energies. The corresponding excess kinetic energies per fragment ion have also been included. It is obvious from the results listed in Table 1 that significant ion losses in our fast-beam apparatus do not occur unless the excess kinetic energy per fragment ion exceeds about 4 eV for the light atomic fragments (F^+, C^+) and 5 eV for the heavier molecular fragments.

(5) We also found that the previously employed method [13,14] of scanning a narrow slit across the entrance cone of the CEM in order to check the spatial collimation of the product ion beam leaving the hemispherical analyzer is not a very reliable way of estimating the total ion loss for two reasons.

(i) The slit, which is typically at ground potential, perturbs the electric field between the analyzer exit and the CEM entrance cone in such a way that the ion trajectories are bent away from the center of the CEM. This tends to overestimate the ion loss suffered in the actual cross section measurement which is carried out without the slit in front of the CEM detector.

(ii) A narrow ion trajectory distribution at the exit of the hemispherical analyzer is not a sufficient indication of the absence of ion losses inside the hemispherical analyzer. Our modeling calculations indicate that under most circumstances the trajectory distribution at the analyzer exit is narrower than the 25 mm diameter of the CEM entrance cone, while nonetheless a significant fraction of ions can be lost earlier along the flight path through the analyzer (see discussion in section (3) above).

Table 1
Ion transmission through the various components of our fast-beam apparatus as predicted by ion trajectory modeling calculations for several two-fragment dissociative ionization processes studied in this work

Process	Total excess kinetic energy (eV)	Excess kinetic energy per ionic fragment (eV)	Ion transmission (%)[a]				
			(a)	(b)	(c)	(d)	(e)
$CF_3 \rightarrow CF_2^+ + F$	1.0	0.28	100	100	100	100	100
	15.0	4.13	100	100	100	100	100
	20.0	5.51	100	100	93	98	91
	30.0	8.26	100	100	72	94	66
$CF_3 \rightarrow CF_2 + F^+$	1.0	0.72	100	100	100	100	100
	5.0	3.62	100	100	100	100	100
	7.0	5.07	100	100	95	100	95
	8.5	6.16	100	100	86	100	86
	14.0	10.14	100	80	40	95	30
$CF_2 \rightarrow CF^+ + F$	1.0	0.38	100	100	100	100	100
	10.0	3.80	100	100	100	100	100
	16.0	6.08	100	100	88	98	86
	20.0	7.60	100	100	82	98	80
$CF_2 \rightarrow CF + F^+$	1.0	0.62	100	100	100	100	100
	6.0	3.72	100	100	100	100	100
	10.0	6.20	100	100	85	100	85
	16.0	9.92	100	96	55	98	51
$CF \rightarrow C + F^+$	1.0	0.61	100	100	100	100	100
	6.0	3.67	100	100	100	100	100
	10.0	6.12	100	100	88	100	88
	15.0	9.30	100	100	72	95	69

For each process, calculations were carried out for several total excess kinetic energies. Also given are the respective excess kinetic energies per ionic fragment in each case according to Eqs. (1a) and (1b). Incident neutral beam energies and all other experimental conditions were chosen to resemble realistic operating conditions in our apparatus.
[a] Calculated ion transmissions through the interaction region (a), the Einzel lens (b), the hemispherical analyzer (c), to the CEM entrance (d), and the total transmission from the interaction region to the CEM detector (e).

Results and discussion

Absolute cross sections were measured for the formation of CF_2^+ and CF^+ fragment ions from CF_3 and for CF^+ ions from the parent CF_2 radical from threshold to 200 eV, with special emphasis on the near-threshold regions of the cross sections. Threshold measurements were carried out first for each fragment ion. A comparison of the measured appearance energy/energies with the thermochemically and spectroscopically determined minimum energy required for the formation of that fragment ion provides an insight into the mechanism(s) through which the ion is formed and gives an indication of the excess kinetic energy released in the dissociation process. Relative cross sections were then measured from threshold to 200 eV. As in the case of the CF_x parent ionization cross sections [10], several individual data sets for each fragment ion had to be combined to improve the statistical quality of the data. For each radical, absolute cross sections for the various fragment ions were obtained relative to the recently published parent ionization cross section [10]. Independent values for all parent ionization cross sections were obtained in the course of this work. They agreed with the recently published cross sections to better than 8%, which is well within

the error margin quoted in the previous paper [10]. Double ionization of the fragment ions was too weak to be measured. With the exception of the formation of F^+ from CF_2 where it was found that two mechanisms contribute to the observed F^+ signal (see discussion below), accurate cross sections for the formation of the atomic fragment ions C^+ and F^+ over the entire energy range could not be obtained due to (i) low signal rates (particularly in the regime of low impact energies below 50 eV) and (ii) the uncertainty in the collection efficiency for these light atomic fragments (see previous discussion). Attempts have been made to provide estimates of the absolute C^+ and F^+ cross sections at 70 eV which we believe are accurate to better than ± 30%.

Dissociative ionization of the CF_3 radical

Figure 4 shows the threshold data for the formation, respectively, of CF_2^+ and CF^+ fragment ions. Each data set was obtained by combining several individual data runs. Each data run was corrected for the contact potential (determined from an onset measurement in Xe) and for possible Rydberg contributions to the ionization signal before the individual data runs were combined. The CF_2^+ threshold data set displays a single onset at 17.1 ± 0.4 eV with little curvature. The thermochemical minimum energy for the formation of $CF_2^+ + F$ from CF_3 is 15.1 ± 0.5 eV [24–27]. We identify the observed onset with this process. The 2 eV energy difference can be accounted for in terms of excess kinetic energy of the dissociating fragments. The excess kinetic energy in this case is distributed between the two dissociating fragments, CF_2^+ and F, according to Eqs. (1a) and (1b), i.e. approximately 0.55 eV for the CF_2^+ ion and approximately 1.45 eV for the neutral F fragment. No

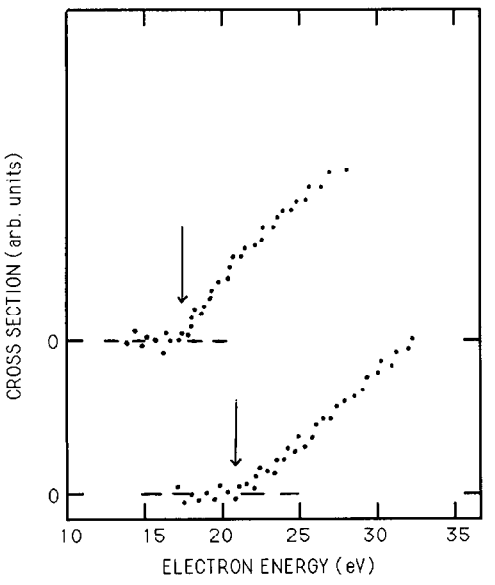

Fig. 4. Ionization threshold for the formation of CF_2^+ fragment ions (top data set) and CF^+ (bottom data set) from CF_3. Both data sets have been obtained by combining several individual data runs (see text for further details). The threshold for each data set has been marked by an arrow.

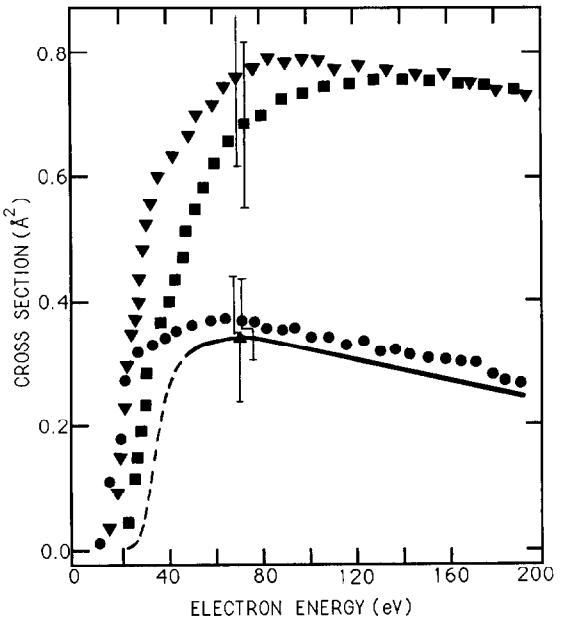

Fig. 5. Absolute electron-impact ionization cross section for the formation of CF_3^+ parent ions (●), and CF_2^+ (▼) and CF^+ (■) molecular fragment ions from CF_3 as a function of electron energy. Also shown (▲) is the absolute cross section for the formation of F^+ atomic fragment ions at 70 eV. The energy dependence of the F^+ cross section is indicated by the solid line above 50 eV and by a broken line below 50 eV which indicates the somewhat tentative nature of the measured energy dependence in that region. The total uncertainty of each of the cross sections is indicated at an impact energy of 70 eV.

evidence was found of an ion signal extending towards lower energies nor did we observe any distinct breaks in the curvature of the cross section in the energy region between threshold and 40 eV. The first finding is indicative of a parent CF_3 neutral radical beam which contains only neutral ground state radicals with little vibrational excitation, which we infer from the absence of any significant curvature in cross section at threshold, and also of the absence of the ion pair formation $CF_2^+ + F^-$, a process which was observed in some cases in the dissociative ionization of the SiF_x ($x = 1$–3) radicals [13–15]. The second observation shows that the positive double ion production $CF_2^+ + F^+$, with a threshold of about 34 eV, does not play a role in the dissociative ionization of CF_3.

The CF^+ threshold data set displays also a single onset at 21.4 ± 0.4 eV and there is little evidence of enhanced curvature. The minimum energy for the formation of $CF^+ + F_2/2F$ from CF_3 is 16.35 ± 0.35 and 17.95 ± 0.35 eV respectively [24–27]. We tend to identify the observed onset with the formation of CF^+ and two fluorine atoms (2F) rather than a fluorine molecule (F_2) based on the smaller energy difference between the required minimum energy for this process and the observed onset. Again, the 3.5 eV energy difference can be accounted for in terms of excess kinetic energy of the dissociating fragments. As before, no evidence was found of an ion signal extending towards lower energies nor did we observe any distinct breaks in the curvature of the cross section up to 40 eV, ruling out the presence of ion pair formation $CF^+ + F^-$ (or $CF^+ + F_2^-$) and double positive ion production $CF^+ + F^+$ (or $CF^+ + F_2^+$).

Figure 5 shows the absolute cross sections for the formation of the two molecular fragment ions CF_2^+ and CF^+ from CF_3 together with the CF_3^+ parent ionization cross section, which is shown for reasons of comparison. Relative cross sections were measured for all ions from threshold to 200 eV. The raw data were corrected for variations in the electron beam current and neutral beam flux and small corrections (less than 5%) were made to the measured shapes below 50 eV and above 150 eV as discussed by Wetzel et al. [21]. The cross section values are also listed in Table 2. At 70 eV, we find absolute cross sections of 0.76 ± 0.15 Å^2 and 0.68 ± 0.14 Å^2 respectively for CF_2^+ and CF^+. Both cross sections are roughly twice as large as that for the parent CF_3^+ ionization [10]. We assign an overall uncertainty of ±20% to the CF_2^+ and CF^+ cross sections, which is slightly larger than the ±18% uncertainty that we determined previously for the CF_3^+ parent ionization cross section [10]. Based on the

Table 2
Cross sections for the ionization of the CF_3 radical by electron impact

Electron energy (eV)	Ionization cross section (Å^2)			
	CF_3^+	CF_2^+	CF^+	F^+
10	0.02	–	–	–
11	0.03	–	–	–
12	0.04	–	–	–
13	0.06	–	–	–
14	0.10	–	–	–
15	0.11	–	–	–
16	0.15	–	–	–
17	0.16	–	–	–
18	0.17	0.06	–	–
19	0.19	0.12	–	–
20	0.20	0.17	–	–
22	0.27	0.25	0.04	–
24	0.30	0.31	0.10	–
26	0.32	0.34	0.15	–
28	0.32	0.40	0.20	
30	0.33	0.49	0.26	–
32	0.33	0.53	0.31	–
34	0.34	0.56	0.34	–
36	0.34	0.59	0.36	–
38	0.35	0.61	0.37	–
40	0.35	0.63	0.40	–
45	0.36	0.65	0.45	–
50	0.36	0.67	0.53	–
55	0.37	0.71	0.58	–
60	0.37	0.72	0.62	–
65	0.38	0.74	0.65	–
70	0.38	0.76	0.68	0.35
80	0.37	0.79	0.70	–
90	0.37	0.78	0.72	–
100	0.35	0.78	0.73	–
120	0.34	0.78	0.75	–
140	0.33	0.77	0.77	–
160	0.32	0.76	0.76	–
180	0.31	0.74	0.74	–
200	0.29	0.73	0.72	–

comparatively small excess kinetic energies in both cases, as inferred from the measured appearance energies, we do not expect any significant ion losses for either the CF_2^+ or the CF^+ signal (see also Table 1). We note that the ordering of the absolute cross sections $\sigma(CF_2^+) > \sigma(CF^+) > \sigma(CF_3^+)$ is similar to observations for the dissociative ionization of SiF_3 by Hayes et al. [14]. The influence of the presence of vibrationally excited parent neutrals in the incident radial beam on the measured cross sections is likely to be small, as discussed in detail by Tarnovsky and Becker [10] in connection with the measurement of the CF_x ($x = 1$–3) parent ionization cross sections.

Also shown in Fig. 5 is the cross section for the formation of the F^+ fragment ion which is indicated by its absolute value of 0.35 Å^2 (±30%) at 70 eV and a solid line representing the energy dependence of the F^+ cross section. Although the F^+ cross section is comparable to the CF_3^+ parent ionization cross section, the F^+ ion signal in the near threshold regime was rather unstable and rendered reliable detailed threshold studies impossible. As a consequence, it was impossible to determine the F^+ threshold to better than a few electronvolts. Based on the threshold data for the other fragment ions from the CF_3 parent radical we do not expect the excess kinetic energy of the F^+ fragment ions to be larger than a few electronvolts per fragment, which would indicate that our apparatus is capable of collecting most of the F^+ fragment ions and that. F^+ ion losses are not a serious problem. As a conservative estimate we put a ±30% uncertainty margin on the reported F^+ cross section from CF_3. The somewhat tentative nature of the F^+ cross section in Fig. 5 in the low energy regime below about 50 eV is indicated by a broken line. We note that no significant ion signal corresponding to the formation of the C^+ fragment ion was observed. Based on the sensitivity of the ion collection and detection system of our fast-beam apparatus we can put an upper limit on the C^+ cross section of 0.1 Å^2 at 70 eV.

The only other measurements of the cross sections for CF_2^+ and CF^+ fragment ion formation

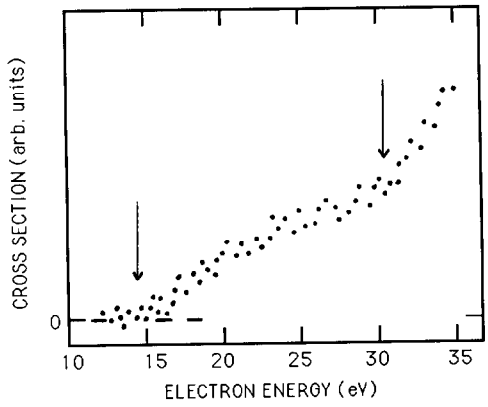

Fig. 6. Ionization threshold for the formation of CF^+ fragment ions from CF_2. The data set has been obtained by combining several individual data runs (see text for further details). The two thresholds corresponding to the two break-up channels $CF_2 \rightarrow CF^+ + F$ (lower threshold) and $CF_2 \rightarrow CF^+ + F^+$ (higher threshold) have been marked by arrows.

from the CF_3 radical are the previous conference reports of this work [11,19,20] and the preliminary studies of Wetzel et al. [17]. Wetzel et al. [17] reported cross sections at 70 eV of 0.7 ± 0.2 Å for CF_2^+ and 0.6 ± 0.2Å for CF^+ which agree with the values reported here to better than 10%, which is well within the combined uncertainty of both measurements.

Dissociative ionization of the CF_2 radical

Figure 6 shows the threshold data for the formation of CF^+ fragment ions. As before, several data runs (each one corrected for contact potential and possible Rydberg contributions) were combined. The data set shows two distinct onsets. The lower onset at 14.6 ± 0.4 eV is very close to the minimum energy of 14.23 ± 0.2 eV [24–27] required for the break-up of a CF_2 radical into a ground-state CF^+ radical and a fluorine atom (F). We assign the lower onset, which displays little enhanced curvature, to this process and note that the amount of excess kinetic energy in the dissociative ionization of the CF_2 radical into a CF^+ ion and a fluorine, F, atom is essentially zero. No ion signal extending to lower impact energies was observed

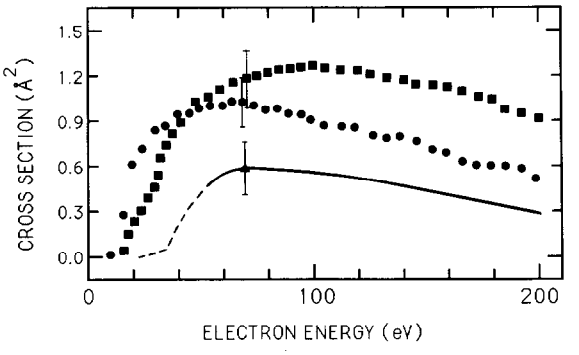

Fig. 7. Absolute electron-impact ionization cross section for the formation of CF_2^+ parent ions (●) and of CF^+ (■) molecular fragment ions from CF_2 as a function of electron energy. Also shown (▲) is the absolute cross section for the formation of F^+ atomic fragment ions at 70 eV. The energy dependence of the F^+ cross section is indicated by the solid line above 50 eV and by a broken line below 50 eV which indicates the somewhat tentative nature of the measured energy dependence in that region. The total uncertainty of each of the cross sections is indicated at an impact energy of 70 eV.

when the CF_2 neutral radical beam was prepared under experimental conditions where essentially no CF_2 metastables were present in the beam (see discussion in ref. 10). The cross section rises smoothly from the first onset for about 17 eV to a distinct break at 31.4 ± 1.0 eV. This second onset is very close to the 31.6 ± 0.2 eV minimum energy for the break-up of the CF_2 radical into CF^+ and F^+. Additional support for the presence of this process and for its contribution to the observed CF^+ ion signal comes from a comparatively large F^+ cross section in the case of the dissociative ionization of CF_2 (compared to CF_3 and CF) with a major onset at the same appearance energy as the second onset observed in the CF^+ cross section (see discussion below).

Figure 7 shows the absolute cross sections for the formation of the molecular fragment ion CF^+ from CF_2 together with the CF_2^+ parent ionization cross section, which is shown for comparison. The relative cross section was measured from threshold to 200 eV. As before, the raw data were corrected for variations in the electron beam current and neutral beam flux and the appropriate corrections to the measured shapes were made (see discussion above).

Table 3
Cross sections for the ionization of the CF_2 radical by electron impact

Electron energy (eV)	Ionization cross section (Å^2)		
	CF_2^+	CF^+	F^+
10	0.05	–	–
11	0.09	–	–
12	0.15	–	–
13	0.18	–	–
14	0.26	–	–
15	0.35	0.04	–
16	0.39	0.09	–
17	0.42	0.13	–
18	0.47	0.18	–
19	0.55	0.20	–
20	0.64	0.23	–
22	0.69	0.31	–
24	0.73	0.36	–
26	0.78	0.40	–
28	0.82	0.43	–
30	0.87	0.48	–
32	0.89	0.62	–
34	0.91	0.74	–
36	0.93	0.80	–
38	0.96	0.84	–
40	0.98	0.88	–
45	0.99	0.97	–
50	1.01	1.02	–
55	1.03	1.08	–
60	1.03	1.11	–
65	1.05	1.16	–
70	1.03	1.19	0.60
80	0.99	1.22	–
90	0.96	1.25	
100	0.91	1.28	–
120	0.86	1.24	–
140	0.78	1.18	–
160	0.67	1.12	–
180	0.58	1.05	–
200	0.49	0.93	–

The cross section values are also listed in Table 3. At 70 eV, we find an absolute cross section of 1.2 ± 0.2 Å^2 for CF^+. The CF^+ cross section is roughly 20% larger than the parent CF_2^+ ionization cross section [10]. We assign the same overall uncertainty of ±16% to the CF^+ cross section that we determined previously for the CF_2^+ parent ionization cross section [10]. Since the measured appearance energy indicated essentially zero

excess kinetic energy we do not expect any ion losses for the CF^+ signal. Although the ordering of the absolute cross sections $\sigma(CF^+) > \sigma(CF_2^+)$ is similar to what was observed for the dissociative ionization of SiF_2 by Hayes et al. [15], we note that the fragment ion cross section exceeded the parent ion cross section by almost a factor of 2 in the case of the SiF_2 radical, which is significantly more than the 20% that we found for CF_2.

As discussed before in connection with the CF^+ threshold data (see Fig. 6), the CF^+ cross section displayed in Fig. 7 clearly shows a break in the slope just above 30 eV which is indicative of a second channel contributing to the total CF^+ signal. The first contribution, with an appearance energy of 14.4 eV, is due to the $CF_2 \rightarrow CF^+ + F$ channel while the second contribution, with an appearance energy of 31.4 eV, can be attributed to the $CF_2 \rightarrow CF^+ + F^+$ channel. Based on the threshold data of Fig. 6 and the overall CF^+ cross section shape shown in Fig. 7, we estimate an absolute cross section of 0.4 Å^2 for the double positive ion pair formation at 70 eV or roughly one third of the total CF^+ cross section at this energy. This estimate assumes a generic "typical" cross section shape for both contributions and takes into account the different appearance energies of the two contributions. We note that Bruce et al. [9] found that the double positive ion formation $CF^+ + F^+$ was also an important channel in the dissociative ionization of the CF_4 molecule, with a cross section of 0.15 Å^2 at 150 eV.

As in the case of the CF_3 parent radical, we also included in Fig. 7 the absolute F^+ cross section at 70 eV (0.60 Å^2) and a solid line representing its energy dependence. As before, we assign the same ±30% margin of uncertainty to the F^+ cross section. Even though the energy dependence of the F^+ cross section below 50 eV is again rather tentative, as indicated by the broken line in Fig. 7, we observed a noticeable increase in the F^+ ion signal around 30 eV which is close to the observed 31.4 eV structure in the CF^+ cross section. The increase in the F^+ ion signal at roughly the same energy lends additional support to the previous interpretation. Based on our earlier estimate of a 0.4 Å^2 cross section for the double positive ion formation $CF^+ + F^+$ from CF_2 at 70 eV, we attribute the remaining 0.2 Å^2 of the measured F^+ cross section of 0.6 Å^2 at 70 eV to the F^+ single positive ion formation. We note that no significant ion signal corresponding to the formation of the C^+ fragment ion was observed and again we put an upper limit of 0.1 Å^2 at 70 eV on the C^+ cross section.

There are no other measurements of the CF^+ and F^+ cross sections from CF_2 with the exception of the previous conference reports of the present work [11,19,20].

Dissociative ionization of the CF radical

The absolute cross section for the parent ionization $CF \rightarrow CF^+$ has been measured before from threshold to 200 eV [10]. The dissociative ionization of this radical produces only weak ion signals for the C^+ and F^+ fragment ions. We measured the F^+ cross section at 70 eV to be 0.25 ± 0.1 Å^2. As before, we can put an upper limit of 0.1 Å^2 (at 70 eV) on the C^+ fragment ion cross section. It was not possible to determine thresholds for the formation of either one of the atomic fragment ions. In the absence of any information regarding the excess kinetic energy with which the C^+ and F^+ ions are formed, it is impossible to determine the fraction of C^+ and F^+ ion that might be lost and remain undetected in our apparatus. A conservative estimate puts that loss at 30% which would correspond to an excess kinetic energy per fragment in excess of 8 eV. Based on this assumption we estimate a combined cross section for the formation of C^+ and F^+ fragment ions from the parent CF radical of 0.35 ± 0.15 Å^2 at 70 eV.

Conclusions

We measured absolute cross sections for the dissociative ionization of CF_3, CF_2 and CF

radicals by electron impact in the energy range from threshold to 200 eV, with peak cross sections of 1.3 Å^2 at 70 eV. For both CF_3 and CF_2, the molecular fragment ionization cross sections (CF_2^+ and CF^+ in the case of CF_3 and CF^+ in the case of CF_2) exceeded the parent ionization cross sections (CF_3^+ and CF_2^+, respectively). In all cases the fragment ions were formed with comparatively small excess kinetic energies ranging from essentially 0 to about 3 eV per fragment. Extensive ion trajectory modeling calculations were carried out in order to quantify the collection efficiency of our fast-beam apparatus for fragment ions formed with excess kinetic energies. The CF^+ cross section from CF_2 displayed two prominent onsets, a lower one corresponding to the formation of $CF^+ + F$ and a higher one representing the double positive ion formation $CF_2 \rightarrow CF^+ + F^+$. The assignment was supported by the comparatively large F^+ cross section in that case (0.6 Å^2 at 70 eV). In all other cases, the F^+ cross sections did not exceed 0.35 Å^2 and cross sections for the formation of the C^+ fragment ions were always found to be less than 0.1 Å^2.

Acknowledgments

We are very grateful to Dr. R.S. Freund and Mr. R.C. Wetzel for many helpful discussions and for their invaluable advice and assistance during the course of this work. Thanks must go to Professor R.A. Bonham for his continued interest in this work and for many stimulating discussions. We further acknowledge Professor H. Deutsch, Professor T.D. Märk, Dr. M. Schmidt and Dr. R. Basner for many stimulating discussions and helpful comments. We appreciate the expert technical support provided by Mr. J. Altmann and his staff in the machine shop and by Mr. Feng Du in the electronics shop. The material presented in this publication is based upon work supported in part by the National Science Foundation through grants CTS-8902405 and CTS-9017211 and by the City University of New York through PSC-CUNY grant 663353. Additional support through a NATO Collaborative Research Grant (CRG-920089) is also gratefully acknowledged. Acknowledgment is also made to the Donors of the Petroleum Research Fund, administered by the American Chemical Society, in partial support of this research through grant 26380-ACS.

References

1 C.J. Mogab, A.C. Adams and D.L. Flamm, J. Appl. Phys., 49 (1978) 3796.
2 C.I.M. Beenakker, J.H.J. van Dommelen and R.P.J. van de Poll, J. Appl. Phys., 52 (1981) 480.
3 I.C. Plumb and K.R. Ryan, Plasma Chem. Plasma Proc., 6 (1986) 205.
4 H. Yabe, A. Yuuki and Y. Matsui, Jpn. J. Appl. Phys., 30 (1991) 2873.
5 U. Müller, T. Bubel, G. Schulz, A. Sevilla, J. Dike and K. Becker, Z. Phys. D, 24 (1992) 131.
6 I. Iga, M.V.V.S. Rao, S.K. Srivastava and J.C. Nogueira, Z. Phys. D, 24 (1992) 111.
7 M.R. Bruce and R.A. Bonham, Int. J. Mass Spectrom. Ion Processes, 123 (1993) 97.
8 H.U. Poll, C. Winkler, V. Grill, D. Margreiter and T.D. Märk, Int. J. Mass Spectrom. Ion Processes, 112 (1992) 1.
9 M.R. Bruce, C. Ma and R.A. Bonham, Chem. Phys. Lett., 190 (1992) 285.
10 V. Tarnovsky and K. Becker, J. Chem. Phys., 98 (1993) 7686.
11 V. Tarnovsky, P. Kurunczi, D. Rogozhnikov, K. Becker, H. Deutsch and T.D. Märk, Verh. Dtschen. Phys. Ges., 28 (1993) 263.
12 SIMION, Version 4.02, Idaho National Engineering Laboratory, EG&G Idaho Inc., Idaho Falls, ID, 1988.
13 F.A. Biaocchi, R.C. Wetzel and R.S. Freund, Phys. Rev. Lett., 53 (1984) 771.
14 T.R. Hayes, R.C. Wetzel, F.A. Biaocchi and R.S. Freund, J. Chem. Phys., 88 (1988) 823.
15 T.R. Hayes, R.J. Shul, F.A. Biaocchi, R.C. Wetzel and R.S. Freund, J. Chem. Phys., 89 (1989) 4035.
16 R.J. Shul, T.R. Hayes, R.C. Wetzel, F.A. Biaocchi and R.S. Freund, J. Chem. Phys., 89 (1989) 4042.
17 R.C. Wetzel, F.A. Biaocchi and R.S. Freund, Bull. Am. Phys. Soc., 30 (1985) 147.
18 H. Deutsch, D. Margreiter and T.D. Märk, Int. J. Mass Spectrom. Ion Processes, 93 (1989) 259.
19 V. Tarnovsky and K. Becker, Bull. Am. Phys. Soc., 37 (1992) 1130.
20 V. Tarnovsky, K. Becker, H. Deutsch and T.D. Märk, Bull. Am. Phys. Soc., 37 (1992) 2009.
21 R.C. Wetzel, F.A. Biaocchi, T.R. Hayes and R.S. Freund, Phys. Rev. A, 35 (1987) 559.
22 R.S. Freund, R.C. Wetzel, R.J. Shul and T.R. Hayes, Phys. Rev. A, 41 (1990) 3575.
23 V. Tarnovsky and K. Becker, Z. Phys. D, 22 (1992) 603.

24 D.D. Wagman, W.H. Evans, V.B. Parker, R.H. Schumm, I. Halow, S.M. Bailey, K.L. Chuney and R.L. Nuttall, J. Phys. Chem. Ref. Data, 11 (suppl. 1) (1982).
25 Ionization Potentials, Appearance Potentials and Heats of Formation of Gaseous Positive Ions, Natl. Stand. Ref. Data, Natl. Bur. Stand. No. 36, Washington, D.C., 1969.
26 S.G. Lias, J.E. Bartmess, J.F. Liebman, J.L. Holmes, R.D. Levine and W.G. Mallard, J. Phys. Chem. Ref. Data, 17 (suppl. 1) (1988).
27 M.W. Chase Jr., K.A. Davis, J.R. Downey, D.J. Frurip, R.A. McDonald and A.N. Syverud, J. Phys. Chem. Ref. Data, 14 (suppl. 1) (1985).